Simulations of Two-Dimensional Foam under Couette Shear

Cox, Simon

Publication date:
2007

Citation for published version (APA):
Cox, S. (2007, Aug 13). Simulations of Two-Dimensional Foam under Couette Shear.
http://hdl.handle.net/2160/323

Simulations of Two-Dimensional Foam under Couette Shear

Simon Cox
Institute of Mathematical and Physical Sciences,
University of Wales Aberystwyth, Ceredigion SY23 3BZ, UK.

July 5, 2007

Abstract

The flow of two-dimensional aqueous foams in the Couette geometry highlights the shear-response of this complex fluid. Quasistatic simulations using the Surface Evolver software are described which allow the calculation of shear stress, bubble velocity, torsion and the location of topolgical changes in teh foam. It is shown that the torsion on the inner cylinder decreases with increasing liquid fraction. After an initial transient the topological changes are located in a region close to the inner cylinder; the width of this region increases with liquid fraction, but is independent of bubble size.

1 Introduction

The flow of foams is seen in many processes, and its use in major industries means that an understanding of the rheology of foams is of paramount importance [1, 2]. Although foams are disordered materials, they have well-defined equilibrium laws which allow their static structure to be determined. It is perhaps the combination of industrial importance with an attractive and precise local structure that makes foams one of the best candidates to improve the understanding of the rheology of multiphase fluids.

A two-dimensional (2D) foam can be made by trapping a foam between two glass plates, for example, and reducing their separation to less than a bubble diameter so that the foam is one bubble thick [3]. The restriction to 2D allows easier visualization of both experiment and simulation: the shape of each bubble can be easily recorded, and its position followed in time, without the need for expensive imaging equipment as in three dimensions. Working with a 2D foam often simplifies the theory, allowing us to isolate and study new phenomena (although we must check for spurious 2D effects).

Minimization of the total film length, subject to constraints such as bubble areas, determines a 2D foam's equilibrium structure, since its energy is proportional to the product of surface tension and film length. The energy of a progressively strained foam increases until a film shrinks to zero length and two three-fold vertices approach one another and undergo a T1 neighbour exchange. These topological changes reduce the total film length and thus the energy; the location and statistics of T1s determines the plastic properties of the foam – in particular its yield stress – and how it releases energy during flow.

Here we examine the flow of a foam in a 2D Couette geometry, in which one of the bounding cylinders is rotated and the other fixed. From the mechanics of a yield stress fluid (consider for example the Bingham model), we expect the shear stress to decrease with the radial position squared. If the fluid has a value of yield stress commensurate with the shear stress then parts of the fluid will yield. As the yield stress decreases, the yielded region will extend further from the inner cylinder (irrespective of which cylinder is rotated). For a foam, this decrease in yield stress might be associated with a higher liquid fraction, and the yielded region is where we expect the T1s to occur.

A 2D foam in a Couette geometry was studied experimentally by Debrégeas et al. [4, 5] and Dennin and co-workers [6–10]. Debrégeas et al. [4] confined the foam between glass plates and slowly rotated the inner cylinder; they find that the T1s are located close to the inner cylinder, and the bubble velocity reduces exponentially as the gap is traversed. In contrast, Dennin slowly sheared a bubble raft (bubbles floating on a liquid surface) and moved the outer cylinder. In this system with higher liquid fraction, the T1s are more widely dispersed and the velocity profile exhibits an obvious change in gradient partway across the gap. The simulations described here suggest that the difference between these two sets of experiments results could be due to the differences in liquid fraction, although simple shear experiments also suggest that the presence of a glass plate bounding the foam has a significant effect on the foam response, even in the quasistatic limit [11], for example through increased drag and lower bubble mobility.

That liquid fraction affects the position of the shear band is perhaps not a surprise, since it is often a significant parameter in foam rheology [12]. There is a difficulty in defining an experimental liquid fraction

that may be compared with the precise measure used in simulations. This is because of the presence of Plateau borders and a meniscus wherever soap films meet walls and liquid surfaces, which means that most experiments are not truly 2D [13].

The cylindrical geometry is thus a determining factor in the localisation of T1s, and a simulation in a rectangular geometry does not explain its presence: in the latter geometry, the band may occur anywhere in the foam [14]. Our aim is to use appropriate simulations to predict the velocity profile and whether or not T1s will localize, given parameters such as bubble and system size, and the liquid content of the foam.

2 Simulation Method

The simulations which follow are in the quasi-static regime, i.e. they allow full relaxation to local equilibrium after each small increment in strain. We use Brakke's Surface Evolver [15], which minimizes the line-length of the foam structure subject to a constraint on each of the bubble areas and incorporates a circular-arc mode, which models soap films precisely rather than as a collection of short straight segments.

A foam's liquid fraction, Φ_l, is its fractional liquid content by volume. For the purpose of simulation, the dry limit of low liquid fraction, $\Phi_l \to 0$, is a natural idealization in which thin films meet in point-like three-fold vertices at 120°. As the liquid fraction increases, the vertices swell into triangular Plateau borders, named after the Belgian scientist who pioneered the study of soap film structures [16]. Instead of incorporating this full description into the simulations that follow, the effect of the non-zero liquid fraction is modelled by a cut-off film length below which T1s are triggered. This mimics the *effect* of the Plateau borders, which cause vertices to touch at a separation greater than a dry model would predict [17].

We use the symmetry capabilities of the Surface Evolver to simulate a sector consisting of $1/16^{th}$ of an annulus of inner radius $r = r_i = 7.1$cm and outer radius $r = r_o = 12.2$cm (figure 1), as in the experiments of [4]. We choose to use a bidisperse foam, since a monodisperse foam would allow the foam to form a crystal ordering with only the innermost bubbles stationary. Those films that meet the inner or outer cylinder have the touching end fixed; this is accomplished in the experiment by using roughened walls, so that they move with that cylinder. We simulate a randomly generated foam with these geometric conditions for at least 400 steps; one step consists in moving the outer cylinder a distance $ds = 0.05$cm and equilibrating the foam. The strain is defined as the distance moved by the outer cylinder, divided by the gap width $r_o - r_i = 5.1$cm. We move the outer cylinder to ensure that there are no numerical artefacts (due to taking too large a step size, for example) that might cause T1s to localize close to the moving cylinder. Moreover, in choosing how to shear the foam we find no qualitative difference between moving just those films attached to the outer cylinder and performing an affine displacement of all bubble vertices before equilibration.

Our control parameter is the cut-off length for T1s, l_c, which is approximately related to a 2D liquid fraction Φ_l by

$$\Phi_l = 0.242 \frac{l_c^2}{\bar{A}}, \tag{1}$$

where $\bar{A}$ is the average bubble area, based upon an assumption that all bubbles are hexagonal. The length l_c is twice the distance from the centre of a triangular Plateau border to an apex where it joins a film, given by Plateau's laws [2, 16]. We use an arbitrary lower limiting value of $l_c = 0.001$. The highest value of l_c that we are able to use is $l_c = 0.075$; larger values cause so many singular four-fold vertices to form that the software is unable to determine how to release ("pop") them to form a foam structure. We are therefore able to access liquid fractions of $5.5 \times 10^{-6} \leq \Phi_l \leq 3.1 \times 10^{-2}$, i.e. up to about 3%. To represent higher liquid fractions in this manner, stable four-fold vertices must be included explicitly, as in the PLAT software [18]. The value of surface tension γ is taken to be one.

3 Results

From each simulation we extract the torsion on the inner cylinder, velocity and stress profiles across the gap, and the locations of the topological changes.

3.1 Shear stress

For a range of values of liquid fraction, the shear stress in the foam was calculated, i.e. the off-diagonal component of the elastic part of the stress tensor (figure 2). This confirms that the stress decreases radially with $1/r^2$. The coefficient of proportionality decreases with increasing liquid fraction, i.e. the foam supports a lower stress when it is wetter.

3.2 Torsion

For each film touching the inner cylinder, we find the angle θ_i of the point of contact with the positive $x-$direction and the angle θ_f of the film with the positive $x-$direction. We assume that the thickness of the 2D system is H and then the torsion is given by

$$T = r_i H \gamma \sum_f \sin(\theta_f - \theta_i) \tag{2}$$

where the sum is over all films f that are anchored to the inner cylinder. To find the stress on the inner cylinder, the torsion should be divided by $2\pi r_i^2 = 316.7\text{cm}^2$ [10].

Measurements of the torsion on the inner cylinder for a foam of $N = 441$ bubbles are shown in figure 3(a). The area ratio between the two bubble sizes is $a_r = \frac{1}{2}$. Each simulation shows an initial transient, which is most pronounced at low liquid fraction. In each case, the torsion increases fairly linearly at the beginning of the simulation, reflecting the elastic response of a dry foam at low strain. For the lowest liquid fraction it then overshoots before coming back to a roughly constant value.

If the direction of strain is reversed after several hundred steps, there is a period of elastic response and then saturation to the same steady state torsion (with a reversed sign) with no overshoot in torsion (figure 3(b)). It therefore appears that the overshoot at the inception of steady shear for foams of low liquid fraction is a consequence of the initial condition, i.e. the starting structure of the foam is trapped in a rather unrealistic state. The data from this early period of strain is thus omitted in the analysis that follows, and lends weight to the importance of pre-shear in experiments and simulations.

By fitting the torsion data for each value of liquid fraction to a horizontal line, we see in figure 4 that the torsion on the inner cylinder decreases with increasing liquid fraction. Increasing the liquid fraction means that bubbles are able to stretch less before a film shrinks below the critical value for a T1. Thus the films pulling on the inner cylinder are shorter at higher Φ_l, and it is reasonable that the torsion should decrease, in the same way that yield stress decreases with increasing Φ_l. A fit to a power-law suggests that the torsion decreases with the square-root of liquid fraction, reflecting the fact that liquid fraction increases with the square of the critical length l_c.

The area ratio between bubbles was varied in the range $0.1 \leq a_r \leq 0.9$. The torsion values do not vary markedly (data not shown), suggesting that the value of 0.5 is representative, and that the significant dependency of the torsion is the liquid fraction. We also checked that the average bubble pressure is essentially constant throughout the foam.

The number N of bubbles was varied in the range $298 \leq N \leq 1088$ while keeping the size of the Couette cell constant. As N increases the average bubble area decreases: $\bar{A} = 19.33/N\text{cm}^2$. The torsion on the inner cylinder increases with N (data not shown) and is commensurate with an affine law.

We confirmed that our results are not affected by (i) sector size, by simulating $1/8^{th}$ of the Couette cell, and (ii) step size, by taking $ds = 0.025$cm, and found no significant differences in the torsion values (data not shown).

Following [19], we compute the frequency and size of the drops in torsion, due to topological changes in the foam. Figure 5 shows that following an increment of strain the torsion drops in about 20% of cases, independent of liquid fraction Φ_l. However, the size of the drop in torsion decreases slightly with increasing liquid fraction – a wetter foam is less able to support larger stresses, since T1 changes reduce the stress. The only exception in the data is that at very low liquid fraction there are many more drops in torsion, with a correspondingly small drop.

3.3 T1 distributions

During the transient, T1s are scattered throughout the foam (figure 6). A further signature of the end of the transient is that the T1s become localized around the inner cylinder [20], as in experiments between glass plates [4] and reminiscent of simulations of simple shear, in which T1s often occur in a system-wide band a fixed distance from the moving cylinder [20]. As many as 30 T1s occur in a given shear step, suggesting system-wide avalanches [14]. Here, we calculate the extent to which T1s are clustered around the inner cylinder, and measure the way in which they spread out as the liquid fraction Φ_l increases.

For $N = 441$, the number of T1s after the transient rises from about 200 to 400 as Φ_l increases (figure 7(a)). The average radial distance of a T1 from the inner cylinder varies little with Φ_l, and most T1s occur with the inner 20% of the gap. However, as the liquid fraction increases a few scattered T1s begin to occur closer to the outer cylinder: figure 7(a) shows the full range of positions, and indicates that T1s can occur anywhere for $\Phi_l > 1\%$. As a measure of this spreading, the figure shows the radial position beyond which less than 1% of T1s occur; this shows a good fit to a curve increasing with $\sqrt{(}\Phi_l)$. We therefore suggest that the region in which T1s are localized spreads with the square-root of liquid fraction.

How does bubble size affect this result? That is, do our foams contain enough bubbles to be sure that we have avoided finite-size effects? Figure 7(b) shows that bubble size does not significantly change the size of the region where T1s occur, even though the number of T1s increases almost linearly in N. Recall that the average bubble area is inversely proportional to the number of bubbles in the Couette cell, so that when N is large the width of the localized region increases *when measured in bubble diameters*. The data in figure 7(b) are all for the same value of the critical length l_c, so that the liquid fraction varies by a factor of 4. However, all data is in the low liquid fraction limit (the plateau in figure 7(a)) so that this should not affect the result.

For a foam of $N = 540$ bubbles, we increased the size of the Couette cell, but not the gap width, using $r_i = 12\text{cm}, \text{r}_\text{o} = 17.1\text{cm}$. There is a slight increase in width of the localized region (data not shown), reflecting the lower curvature of the cylinders and thus the lower shear stresses present.

3.4 Velocity

A further measure of the transient is obtained from the velocity profile in the annulus. We show in figure 8 the azimuthal bubble displacement, both as the change in angle $\Delta\theta$ that the centre of a bubble subtends at the centre of the cylinder, normalized by the change in angle of a point on the moving outer cylinder, and the distance moved $r\Delta\theta$ (inset), normalized by the distance moved by the outer cylinder, plotted against radial position. Data are averaged over twenty intervals in the radial direction and over shear steps both before and after the transient, for two values of liquid fraction. As for the torsion measurements, the steady-state velocity is an average over all steps after the transient ends.

For each value of liquid fraction, the profile in the transient, the period when T1s occur throughout the foam, is roughly linear. Once the T1s localize close to the inner cylinder, the bubbles close to the inner cylinder remain stationary, most obvious at low liquid fraction, and bubbles outside the localized region deform elastically. There is a narrow region, the width of which increases with liquid fraction, separating the stationary region from the elastic region.

4 Conclusion

We have used bubble-scale simulations to probe the response of a foam in a 2D Couette viscometer. We find that (i) the shear stress decreases quadratically across the gap, as expected from continuum considerations; (ii) at low liquid fraction the initial structure of a simulated foam can give misleading overshoots in, for example, the torsion response, presumably due to severely distorted bubbles; (iii) the torsion on the inner cylinder decreases with the square-root of the liquid fraction of the foam; (iv) T1s localize close to the inner cylinder, and the width of the localized region increases with liquid fraction, with the possibility (e.g. at high liquid fraction and small inner radius) that it extends to cover the whole system; (v) the width of the localized region depends upon the dimensions of the Couette cell but not upon bubble size.

We have neglected the effects of viscous dissipation. In slow Couette shear experiments, viscosity should not be too important, but the effect of friction with the glass plates will, in the future, be tested explicitly using the viscous froth model of Kern et al. [21]. These results may also be applicable to the flow of three-dimensional foams in a Couette viscometer [22]; if this is the case it would indeed be serendipitious, since 3D simulations remain a challenge.

Acknowledgements

The author thanks K. Brakke for assistance with the Surface Evolver software, F. Graner, M. Dennin and A. Kraynik for many useful discussions and their comments on an early draft, and B. Dollet and D. Weaire for useful suggestions. He thanks LSP Grenoble for hospitality during part of the period when this work was developed. Financial support is acknowledged from the University of Wales Aberystwyth Senate Fund, the Ulysses France-Ireland Exchange Scheme and EPSRC (EP/D014956/1, EP/D048397/1, EP/D071127/1).

References

[1] A.M. Kraynik. Foam flows. *Ann. Rev. Fluid Mech.*, **20**:325–357, 1988.

[2] D. Weaire and S. Hutzler. *The Physics of Foams.* Clarendon Press, Oxford, 1999.

[3] S.J. Cox, D. Weaire, and M.F. Vaz. The transition from two-dimensional to three-dimensional foam structures. *Eur. Phys. J. E*, **7**:311–315, 2002.

[4] G. Debrégeas, H. Tabuteau, and J.M. di Meglio. Deformation and flow of a two-dimensional foam under continuous shear. *Phys. Rev. Lett.*, **87**:178305, 2001.

[5] E. Janiaud and F. Graner. Foam in a two-dimensional Couette shear: a local measurement of bubble deformation. *J. Fluid Mech.*, **532**:243–267, 2005.

[6] M. Dennin. Statistics of bubble rearrangements in a slowly sheared two-dimensional foam. *Phys. Rev. E*, **70**:041406, 2004.

[7] C. Gilbreth, S. Sullivan, and M. Dennin. Flow transitions in two-dimensional foams. *Phys. Rev. E*, **74**: 051406, 2006.

[8] J. Lauridsen, M. Twardos, and M. Dennin. Shear-induced stress relaxation in a two-dimensional wet foam. *Phys. Rev. Lett.*, **89**:098303, 2002.

[9] J. Lauridsen, G. Chanan, and M. Dennin. Velocity profiles in slowly sheared bubble rafts. *Phys. Rev. Lett.*, **93**:018303, 2004.

[10] E. Pratt and M. Dennin. Nonlinear stress and fluctuation dynamics of sheared disordered wet foam. *Phys. Rev. E*, **67**:051402, 2003.

[11] Y. Wang, K. Krishan, and M. Dennin. Impact of boundaries on velocity profiles in bubble rafts. *Phys. Rev. E*, **73**:031401, 2006.

[12] C. Raufaste, B. Dollet, S.J. Cox, F. Graner, and Y. Jiang. Yield drag in a two-dimensional foam flow around a circular obstacle: the role of fluid fraction. *Euro. Phys. J. E*, **(in press)**:?–?, 2007.

[13] M.F. Vaz and S.J. Cox. Two-bubble instabilities in quasi-two-dimensional foams. *Phil. Mag. Letts.*, **85**: 415–425, 2005.

[14] Y. Jiang, P.J. Swart, A. Saxena, M. Asipauskas, and J.A. Glazier. Hysteresis and Avalanches in two-dimensional foam rheology simulations. *Phys. Rev. E*, **59**:5819–5832, 1999.

[15] K. Brakke. The Surface Evolver. *Exp. Math.*, **1**:141–165, 1992.

[16] J.A.F. Plateau. *Statique Expérimentale et Théorique des Liquides Soumis aux Seules Forces Moléculaires*. Gauthier-Villars, Paris, 1873.

[17] S.J. Cox. The mixing of bubbles in two-dimensional foams under extensional shear. *J. Non-Newtonian Fl. Mech.*, **137**:39–45, 2006.

[18] S. Hutzler, D. Weaire, and F. Bolton. The effects of Plateau borders in the two-dimensional soap froth III. Further results. *Phil. Mag. B*, **71**:277–289, 1995.

[19] M. Twardos and M. Dennin. Comparison between step strains and slow steady shear in a bubble raft. *Phys. Rev. E*, **71**:061401, 2005.

[20] S.J. Cox, D. Weaire, and J.A. Glazier. The rheology of two-dimensional foams. *Rheol. Acta*, **43**:442–448, 2004.

[21] N. Kern, D. Weaire, A. Martin, S. Hutzler, and S.J. Cox. Two-dimensional viscous froth model for foam dynamics. *Phys. Rev. E*, **70**:041411, 2004.

[22] S. Rodts, J.C. Baudez, and P. Coussot. From "discrete" to "continuum" flow in foams. *Europhys. Lett.*, **69**:636–642, 2005.

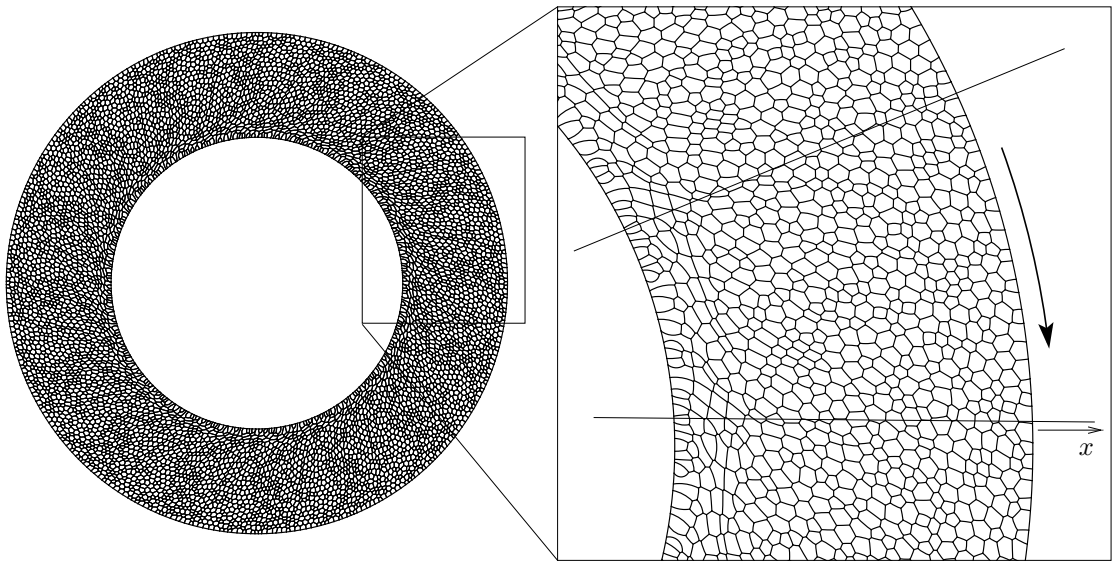

Figure 1: The outer cylinder of one-sixteenth of a Couette viscometer is rotated in small increments (quasi-static limit) to strain a foam. There are periodic boundary conditions in the azimuthal direction, as indicated, with 441 bubbles in the unit cell, and therefore $16 \times 441 \approx 7 \times 10^3$ bubbles in total.

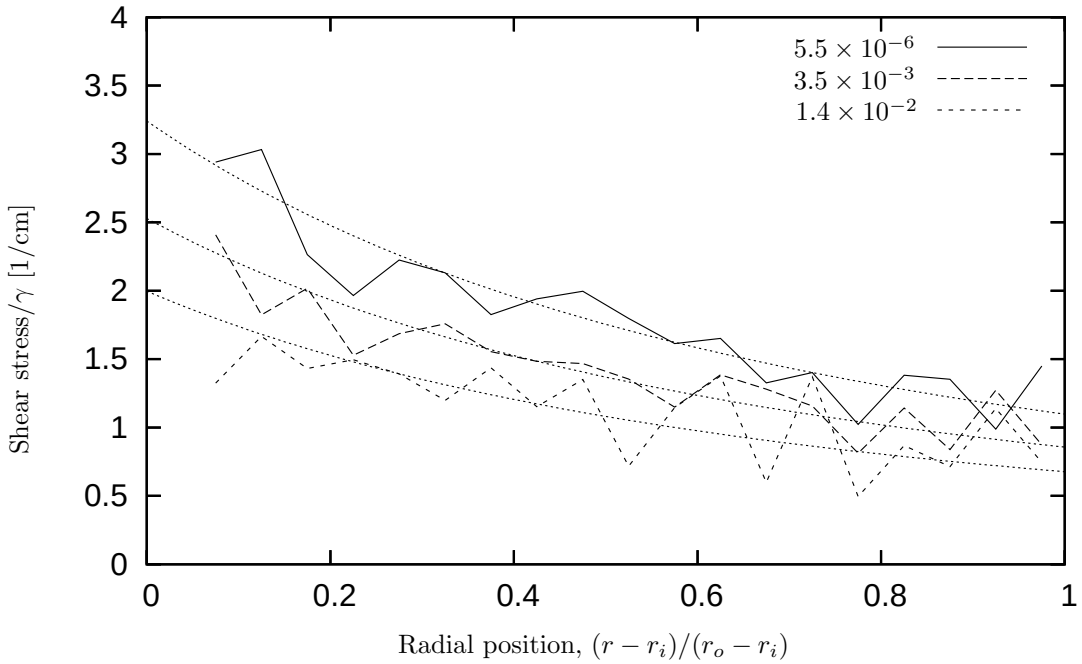

Figure 2: The shear stress in the foam, averaged over all films and all steps after the transient ($N = 441$). For each value of liquid fraction Φ_l, the stress decreases as $a(\Phi_l)/r^2$ (dotted lines) for a constant a that decreases with increasing Φ_l.

(a)

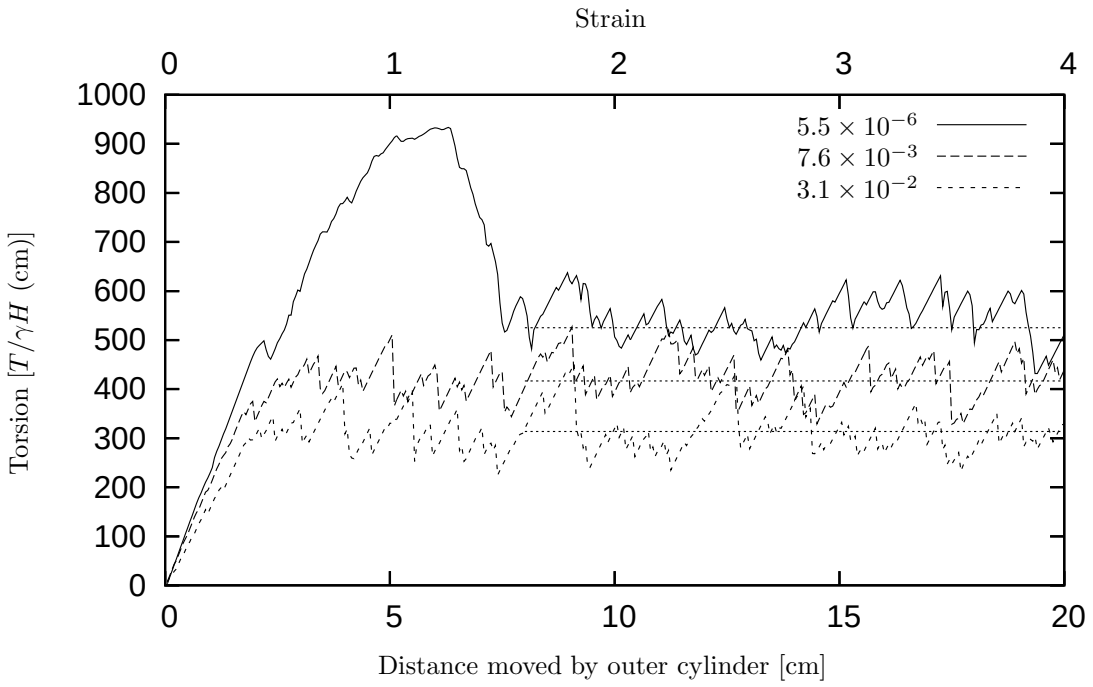

(b)

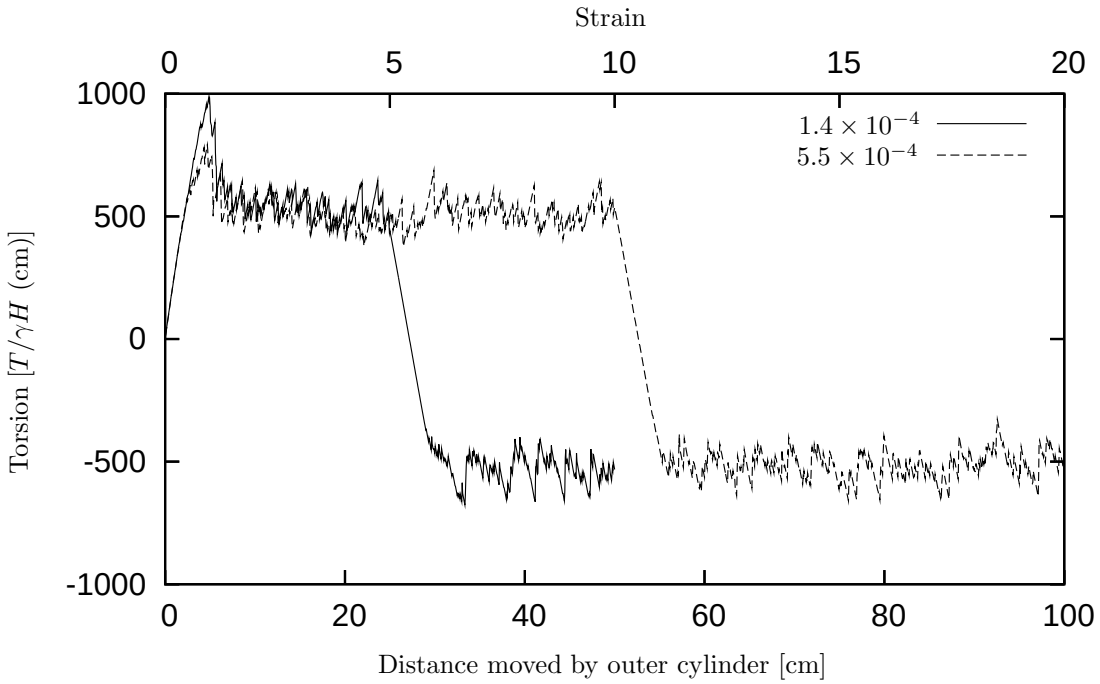

Figure 3: The torsion on the inner cylinder when the outer cylinder is slowly rotated. The value obtained in these simulations of $N = 441$ bubbles is multiplied by 16 to account for the whole annulus. (a) Three representative liquid fractions. There is an initial transient, most apparent for the lowest liquid fraction, which lasts up to a strain of about 1.6. This value is taken as the end of the transient for all subsequent analysis – horizontal lines show the fitted plateaux. (b) Reversing the direction of rotation after the steady-state has been reached indicates that the overshoot in torsion only occurs when the foam is first sheared. Two results are shown, for different liquid fractions and different maximum strains. There is a period of elastic response when the direction is first reversed.

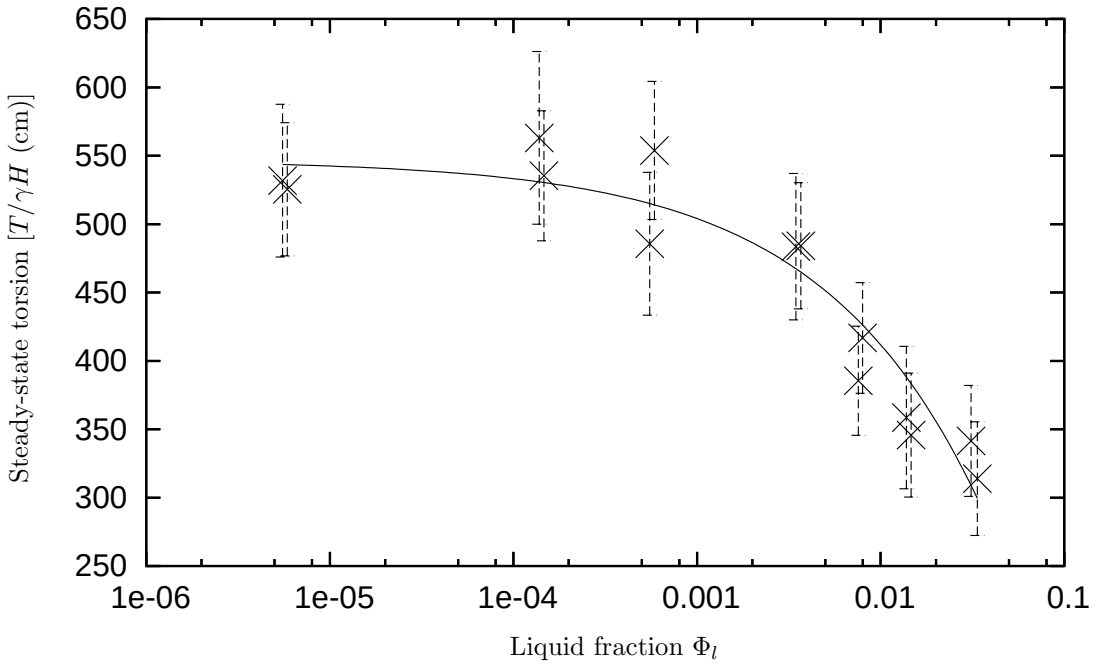

Figure 4: The steady-state torsion decreases with the square-root of liquid fraction (solid line) in the form $T = \gamma H(a_T - b_T\sqrt{\Phi_l})$, with $a_T = 547$cm and $b_T = 135$cm. Two simulations ($N = 441$) were performed for each value of Φ_l, and the abscissa of one value shifted slightly for clarity.

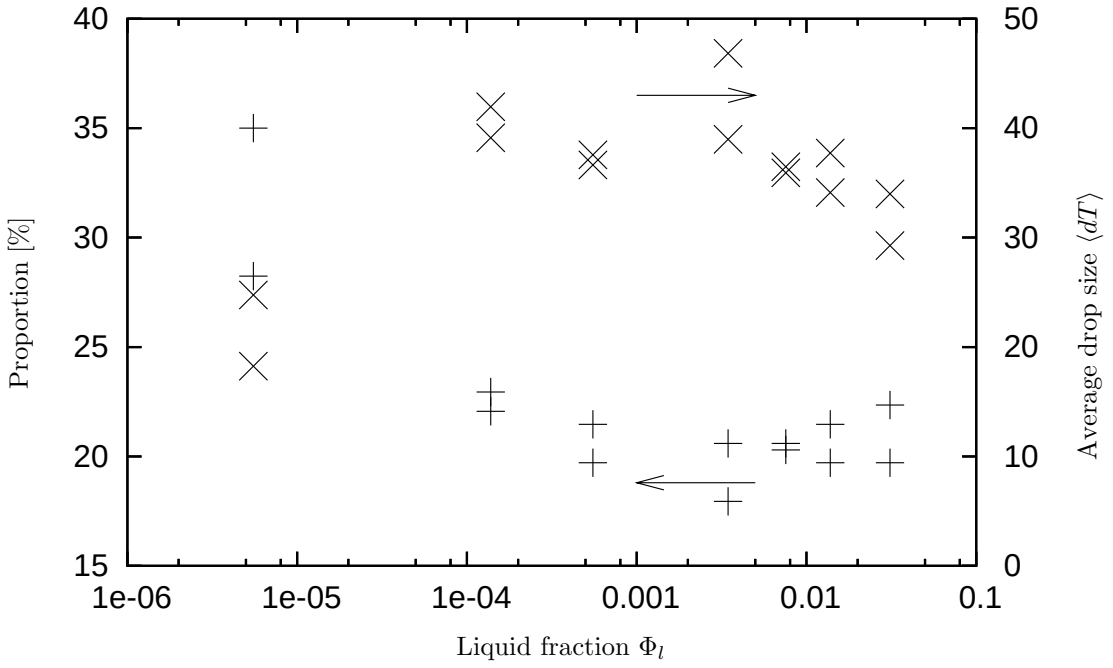

Figure 5: For a foam of $N = 441$ bubbles, about 20% of iterations result in a drop in the torsion on the inner cylinder, increasing slightly at lower liquid fraction. The average drop in torsion decreases with increasing liquid fraction, with the exception of two anomalous points at very low liquid fraction.

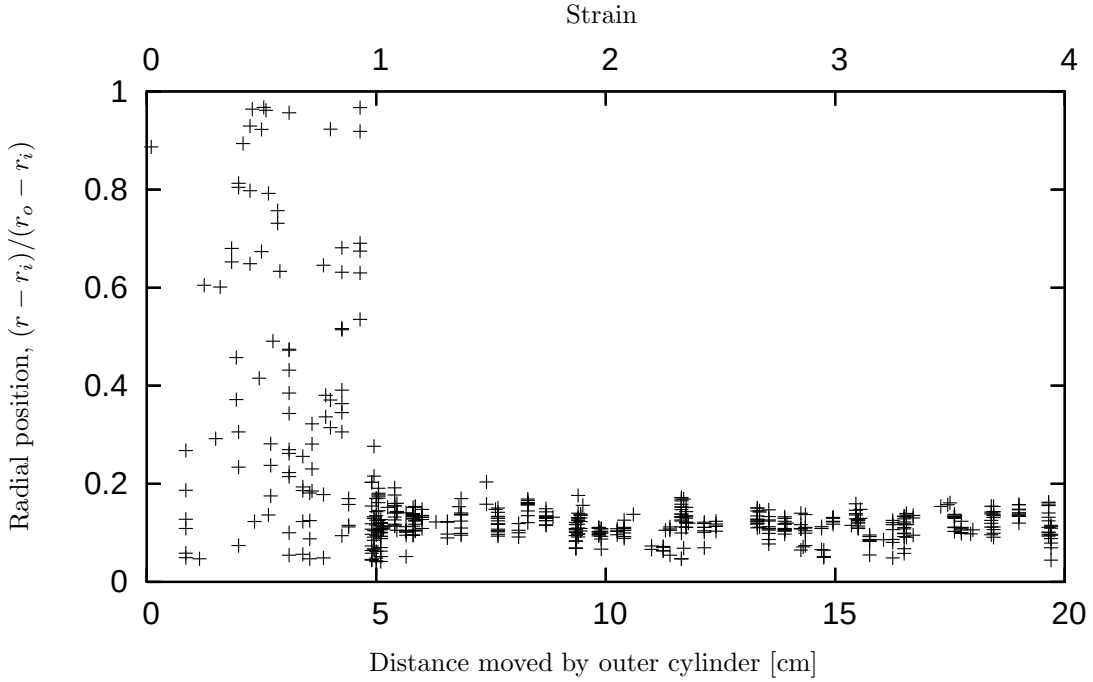

Figure 6: The radial position of each T1 ($N = 441, l_c = 0.1$) as strain increases. Above about unit strain the T1s only occur close to the inner cylinder. Many T1s can occur at each step in strain.

(a)

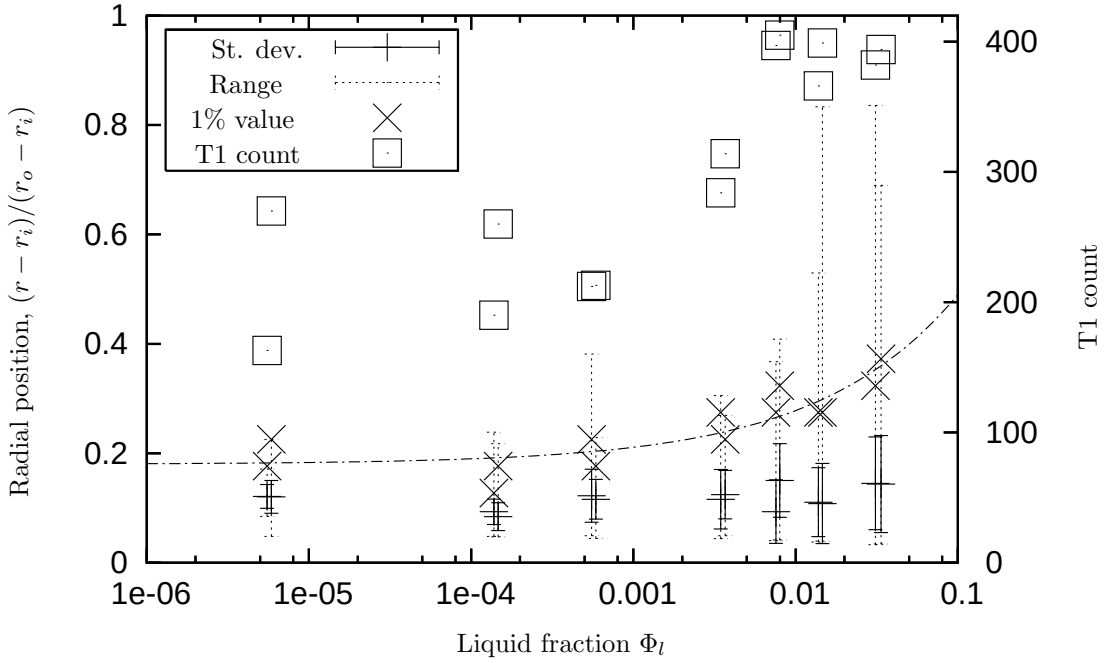

(b)

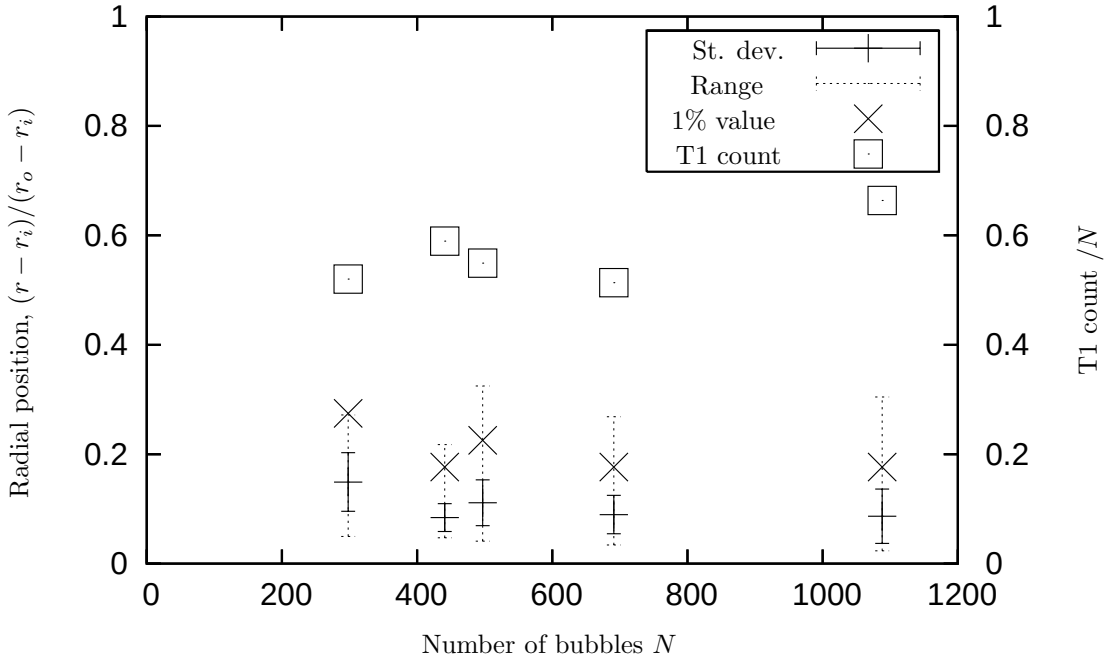

Figure 7: (a) The radial distribution of T1 topological changes after the transient for $N = 441$. The graph shows the range of positions of the T1s, as well as the mean position and standard deviation, and the position beyond which less than one percent of T1s occur. The dot-dashed line is a fit to this latter data, $0.18 + 0.98\sqrt{\Phi_l}$. Also, the number of T1s rises from about 200 to 400 as Φ_l increases. (b) The number of bubbles N in the foam, and equivalently the average bubble size, does not affect the position where T1s occur (with $l_c = 0.005$, i.e. $\Phi_l = 1.4 \times 10^{-4}$). However, the total number of T1s that occur increases approximately linearly with N.

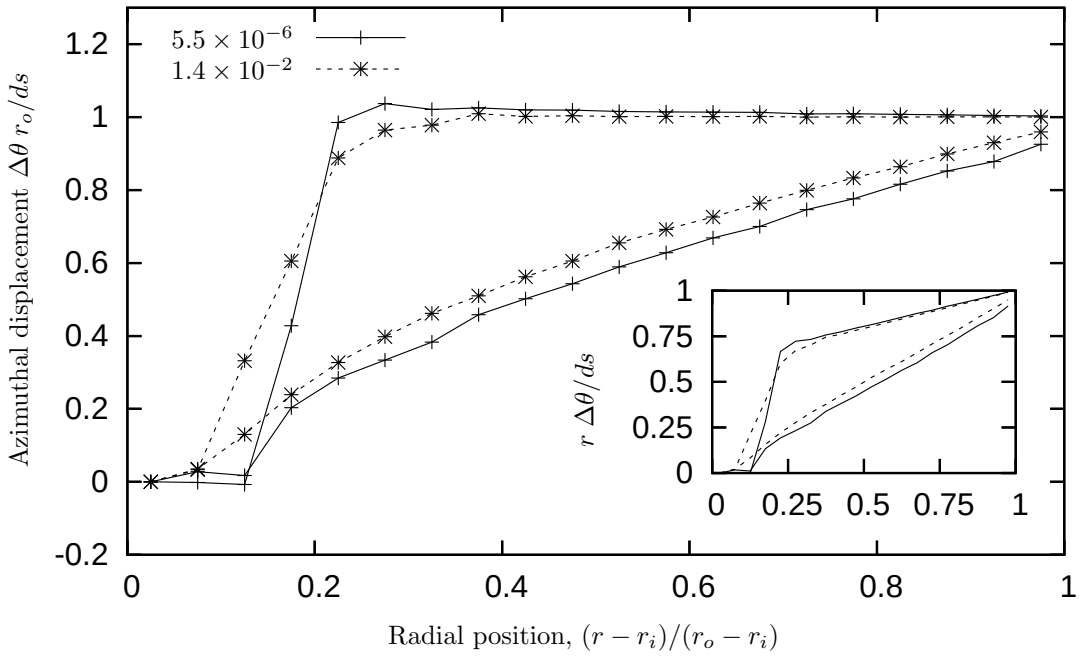

Figure 8: The azimuthal bubble displacement and distance moved (inset), for two values of liquid fraction, representing the velocity profile across the gap ($N = 441$). The data is binned into 20 radial intervals at the beginning of the transient (lower lines) and after it. Initially the deformation is almost linear, with bubbles moving in proportion to their distance from the inner cylinder. In the steady regime the profile changes to one in which the outer bubbles move elastically with the outer cylinder, the inner bubbles are stationary and there is a transition over a short distance to connect the two.